Phospholipid Membranes

DOI: 10.1002/ange.201406927

Internalization of Silica Nanoparticles into Fluid Liposomes: Formation of Interesting Hybrid Colloids**

Raphael Michel, Ellina Kesselman, Tobias Plostica, Dganit Danino, and Michael Gradzielski**

Abstract: *The formation of hybrid materials consisting of membrane-coated silica nanoparticles (SiNPs) concentrated within small unilamellar vesicles (SUVs) of 1,2-dioleoyl-sn-glycero-3-phosphocholine (DOPC) is described. They are formed by a simple self-assembly process resulting from invagination of the SiNPs into the SUVs and subsequent vesicle fusion, thereby retaining an almost constant size. This process was followed under conditions where it proceeds slowly and could be analyzed in structural detail. The finally formed well-defined SiNP-filled vesicles are long-time stable hybrid colloids and their structure is conveniently controlled by the initial mixing ratio of SiNPs and vesicles.*

The interaction of phospholipid membranes with nanoparticles (NPs) is a central aspect for understanding nanotoxicity, and therefore is currently investigated intensely because of the increased use of NPs and growing concerns regarding their health impact. Furthermore this interaction and the transport through membranes is very important for applications of NPs as delivery or imaging systems. In that context, many studies focused on interactions in mixed systems of phospholipid membranes (e.g. vesicles as model systems) and inorganic NPs.[1] Such mixtures are not only important as models for studying the biological impact of NPs but also as interesting route for creating new colloidal hybrid materials that combine the softness of vesicles with the hard colloid properties of inorganic NPs.

We investigated mixtures of phospholipid vesicles (liposomes) that resemble biological membranes, and small silica nanoparticles (SiNPs), with the particular aim to study how the transport of nanoparticles through the membrane and into the vesicle interior proceeds and what structures are formed during this process. As phospholipid we employed DOPC (1,2-dioleoyl-sn-glycero-3-phosphocholine) with its phase transition temperature at −18 °C,[2] thus forming fluid membranes at room temperature. Attractive interactions between the fluid zwitterionic liposomes and the hydrophilic NPs are expected to prevail because of the generally high Hamaker constant for silica and phospholipids and specific interactions between the head group and silica.[3] Such strong attraction results in binding of the SiNPs to the lipid and constitutes the driving force for internalization in a process analogous to endocytosis (see Figure 1), where particles become covered with a supported lipid bilayer (SLB) during the internalization process.[4]

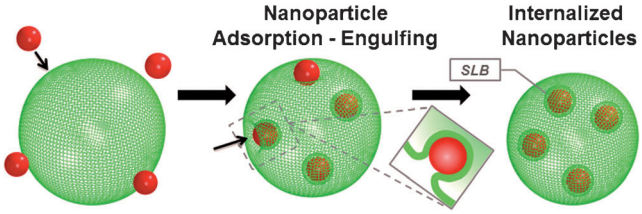

Figure 1. Scheme depicting the mechanism of NP internalization. Hydrophilic NPs adsorb to the lipid are wrapped and finally internalized into the fluid liposomes, thereby forming supported lipid bilayer (SLB) NPs (the inset depicts the process of invagination).

This process depends on the balance between adhesion energy per unit area, W, and the bending energy (described by Helfrich[5] by the mean bending modulus κ of the DOPC membrane) required to form a SLB around the SiNPs. Incorporation will proceed if the adhesion energy between particles and membrane is higher than the energy costs associated with the bending of the membrane around the curved particle surface. This is only possible if the particle radius is larger than a critical value [R_C; Eq. (1)].[6]

$$R_c \equiv \sqrt{2\kappa/|W|} \qquad (1)$$

Previous work estimated the critical particle radius [Eq. (1)] to be in the range of 10–15 nm.[4] This value was obtained with cryo-TEM, observing the presence or absence of internalized particles in samples containing DOPC vesicles and SiNPs of decreasing size. Considering that the bending modulus of a DOPC bilayer is typically around $\kappa \approx 8\text{–}10 \times 10^{-20}$ J ($\approx 20\text{–}25\ kT$) at room temperature,[7] this corresponds to an adhesive strength (W) in the range of 0.7–1.6 mJ m^{-2}, comparable to usual interfacial energies.[8]

Systematic investigations of such mixed systems are important but so far have not been done in a comprehensive

[*] Dr. R. Michel, T. Plostica, Prof. Dr. M. Gradzielski
Stranski-Laboratorium für Physikalische und Theoretische Chemie
Institut für Chemie, Technische Universität Berlin
10623 Berlin (Germany)
E-mail: michael.gradzielski@tu-berlin.de
r.michel3@hotmail.fr
Dr. E. Kesselman, Prof. Dr. D. Danino
Department of Biotechnology and Food Engineering
Technion, Haifa, 32000 (Israel)

[**] Financial support by the German Research Foundation (DFG) in the framework of the IGRTG 1524 (SSNI) is gratefully acknowledged. For instructive discussions we thank Dr. T. Weikl, Dr. A. Bahrami, and J. Agudo. The support of the Russell-Berrie Nanotechnology Institute and the Israel Science Foundation are highly acknowledged. D.D. also wants to thank the COST1101 action for support.

Supporting information for this article is available on the WWW under http://dx.doi.org/10.1002/anie.201406927.

fashion. Apart from size-dependent incorporation studies,[4] investigations were done on the uptake of hydrophilic NPs by polymersomes[9] which have the advantage of enhanced mechanical stability but are quite different to biologically relevant phospholipid-based membranes. Combining phospholipids and SiNPs also allows to form NP/membrane hybrids.

Accordingly we studied well-defined mixtures of zwitterionic DOPC liposomes and small SiNPs in aqueous solution. Unilamellar vesicles of a hydrodynamic radius of 58 nm (dynamic light scattering) were obtained by subsequent extrusion (for details see the Supporting Information). Dynamic light scattering (DLS) showed a polydispersity index (PDI) of 0.1 whereas small-angle neutron scattering (SANS; Figure S2) confirmed this size but gave a larger apparent PDI of 0.24, which is more realistic (see the Supporting Information). To the vesicle solutions previously dialyzed SiNPs of $R_{NP} \approx 8$ nm were added and slowly mixed under stirring. The lipid concentration was kept constant at 0.1 wt% (1.27 mM), while the NP concentration ranged from 0 to 0.085 wt%. We varied systematically the concentration ratio [NP]/[vesicle] to see how this affects the structure of the formed hybrid systems. As an additional normalized concentration we introduce the ratio β, the amount of bilayer required for complete formation of SLBs around the SiNPs with respect to the initially available vesicle bilayer (for details see the Supporting Information). In other words, β is the relative amount of membrane consumed by the NPs upon internalization. By choosing the size of the SiNPs to be around the estimated critical radius one may expect the incorporation to proceed slowly, so successive invagination steps of this process can be well monitored.

The macroscopic phase behavior of 0.1 wt% DOPC vesicle samples and different SiNP concentrations was visually inspected for several months (22 ± 2 °C). Photographs at various time points (Figure S3) show that immediately after preparation all samples look similar to the initial vesicle dispersion. After 10 days, systems containing small quantities of SiNP are significantly more turbid (see samples with [NP]/[vesicle] of 4.2 and 11.8 in Figure S3), indicating that aggregation or fusion processes have taken place. In contrast, the pure vesicle solution and the mixed systems containing higher particle concentrations remain similarly transparent after this time, as they were shortly after preparation. The stability of the pure DOPC vesicle system is due to the repulsive steric forces caused by curvature fluctuations of the fluid membrane (undulation forces).[13]

These results are similar to observations reported for comparable mixed systems containing gel-state bilayer vesicles (dipalmitoylphosphatidylcholine, DPPC, at room temperature).[10] In that case, the rigidity of the gel membrane, having a bending modulus (κ) around 120×10^{-20} J (about 300 kT),[11] prevents SiNP transport through the bilayers. The instability observed for low SiNP content results from the presence of just a few adsorbed particles that introduce an attractive interaction, thereby bridging neighboring liposomes.[10,12] In contrast, the higher stability found for larger NP concentrations was attributed to the adsorption of a sufficiently high amount of charged NPs onto the vesicle surface, thereby introducing repulsive interactions between those SiNP-decorated vesicles.

The observations in our system of fluid liposomes may be similarly explained. As the SiNP radius is close to the critical radius R_C [Eq. (1)], the driving force for particle internalization is low. Hence, the SiNPs remain for a long time on the outer surface of the vesicles, leading to a behavior similar to that observed with gel-like liposomes. Accordingly, long-time colloidal stability (little changes in the first 10 days) of the liposomes was observed for [NP]/[vesicle] ratios larger than 14. In contrast, for our concentration range of interest, which is below the point of potential complete bilayer consumption, namely [NP]/[vesicle] < 14 ($\beta < 1.0$), substantial changes are seen already after relatively short times (Figure S3).

To get a more quantitative insight, these changes were followed by static and dynamic light scattering, where static light scattering (SLS; Figure 2B) monitors the effective molecular mass of the dispersed aggregates (vesicles and bound or incorporated SiNPs) while DLS (Figure 2A) measures their geometric size by the hydrodynamic radius R_h (experiments were repeated three times confirming reproducibility). One finds that initially R_h decreases, while the scattering intensity R_θ remains rather constant (Figure 2; R_θ does not depend on the amount of added SiNPs as their scattering contribution is much less than that of the vesicles). This can be interpreted such that the total mass of the vesicle/SiNP aggregates does not change but they become smaller

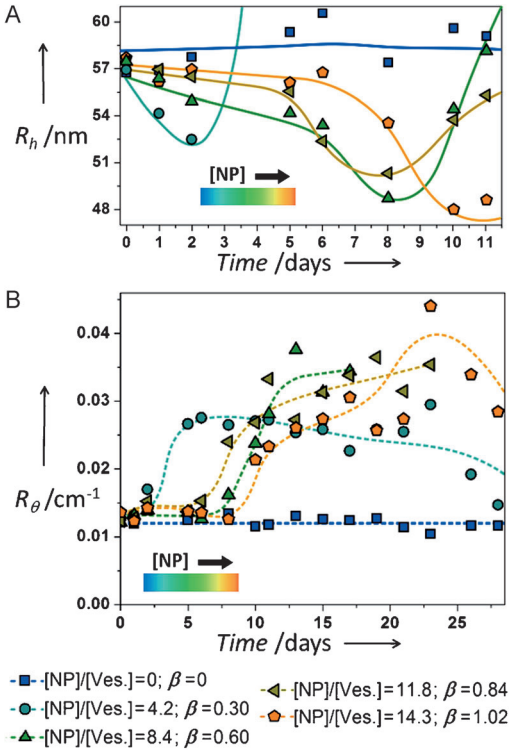

Figure 2. Light scattering results for mixed DOPC/SiNP samples for different [NP]/[vesicle] ratios as a function of time. A) Hydrodynamic radius R_h and B) Raleigh ratio R_θ at 90°.

because of the incorporation of the SiNPs that consumes bilayer material. After R_h passes through a minimum, both, R_h and R_0, increase substantially and then remain constant for longer times (Figure 2). This increase of size and scattering intensity can be attributed to the fusion of vesicles (a large increase seen by DLS in Figure S4A for longer times can be attributed to the formation of agglomerates but not to larger individual vesicles). These processes occur faster for lower [NP]/[vesicle] ratios. Apparently, in the case of higher concentrations of SiNPs, the larger amounts of adsorbed SiNPs stabilize the vesicles electrostatically,[10] thereby delaying the process of fusion responsible for the increase in R_h. In contrast, the pure DOPC dispersion ($\beta = 0$) shows almost no changes during the observation period of four weeks since the fluid vesicles are stabilized by undulation forces.[13] Of course, light scattering does not yield a detailed structural picture, but gives reliable insights into the changes going on as a function of time.

The incorporation of a number N_p of SiNPs according to Figure 1 leads to a systematic reduction of the vesicle size from an initial value $R_{V,0}$ to a final value of $R_V(n_p)$, since during invagination a corresponding amount of vesicle bilayer is consumed for the formation of SLB surrounding the incorporated SiNPs. Assuming perfectly spherical vesicles, this new radius is given by Equation (2),

$$R_V(N_p) = \sqrt{R_{V,0}^2 - N_p(R_{NP} + \Delta)^2} \quad (2)$$

where R_{NP} is the SiNP radius and Δ the distance of the SLB midplane from the surface of the SiNPs. For our case of initial vesicles with $R_{V,0} = 58$ nm the incorporation of 4 (8) NPs ($R_{NP} = 8.1$ nm and $\Delta = 2.6$ nm) yields a radius of $R_V(n_p{=}4(8)) = 53.9$ (49.5) nm. Comparison with the data shown in Figure 2 shows that such incorporation of about 4–8 SiNPs into DOPC vesicles explains well the initially observed reduction of the vesicle size and the characteristic time of incorporation is 1–5 days. Incorporating larger numbers of SiNPs would lead to quite small vesicles and the only escape of the hybrid system to such curvature constraints is possible by fusion of vesicles.

This interpretation was confirmed by cryo-TEM experiments[14] that show for an [NP]/[vesicle] ratio of 4.2 after three weeks similarly sized vesicles of $R \approx 60$ nm with internalized SiNPs (Figure 3; Figure S5 shows pure DOPC vesicles). On average one finds 6.3 encapsulated SiNPs in vesicles with $\langle R \rangle = 57$ nm (for quantitative interpretation of the cryo-TEM images we always analyzed about 40–70 vesicles, see Figure S6). This corresponds to an average fusion of 1.5 vesicles, if one assumes all SiNPs to be incorporated (in agreement with cryo-TEM, which shows basically no free SiNPs).

For the case of having the larger [NP]/[vesicle] ratio of 8.4 we find by cryo-TEM somewhat larger vesicles of $\langle R \rangle =$ 67 nm, where the SiNPs are in a relatively densely packed state (Figure 4). Of course, this means that for the formation of these interesting hybrid colloids a number of vesicles must have fused in order to provide the bilayer material both for the SLB of the internalized SiNPs (as they now have consumed 60 % of the initially present phospholipid bilayer) and for retaining the vesicle size. From analyzing the cryo-TEM data we can conclude that on average 26.4 SiNPs are contained per vesicle, which then means that about 3.2 vesicles must have fused for their formation.

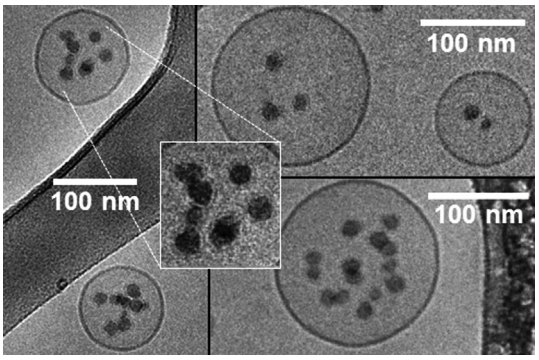

Figure 3. Cryo-TEM micrographs of samples with [NP]/[vesicles] = 4.2 ($\beta = 0.30$) taken three weeks after sample preparation. The enlargement shows the presence of SLBs around internalized SiNPs.

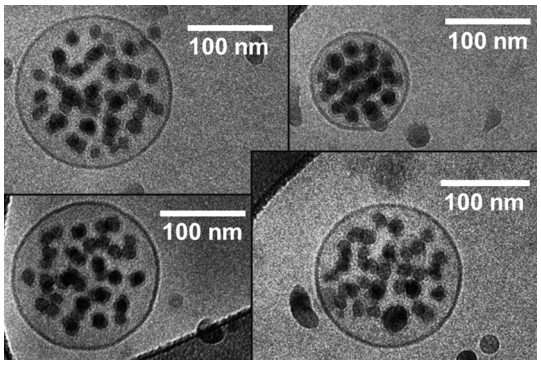

Figure 4. Cryo-TEM micrographs of samples with [NP]/[vesicle] = 8.4 ($\beta = 0.60$) taken three weeks after sample preparation.

The structural evolution of the hybrid aggregates in the SiNP/DOPC system is summarized in Figure 5. Initially, the strongly adsorbed SiNPs become slowly incorporated into the vesicles, as the size of our SiNPs is close to the critical radius R_C [Eq. (1)]. Because of the strong attraction between silica and DOPC, they cover themselves in this process by a lipid bilayer (SLB), thereby consuming a part of the lipid membrane, which leads to a corresponding decrease of the average vesicle size [described by Eq. (2)]. This process is slower the larger the SiNP content is because adsorbed particles in the neighborhood hinder the invagination process. The SLB-covered SiNPs no longer have a tendency for attaching to the vesicle membrane and are now entrapped within the vesicles. However, this process of incorporation can proceed only to a certain extent as then increasingly curved vesicles are formed that are disfavored by the bending energy.

Now a second elementary process—vesicle fusion—takes place on a time scale of days as seen by light scattering and cryo-TEM (without SiNPs, the vesicle size remains unchanged, see Figure 2). Fusion is catalyzed by the presence

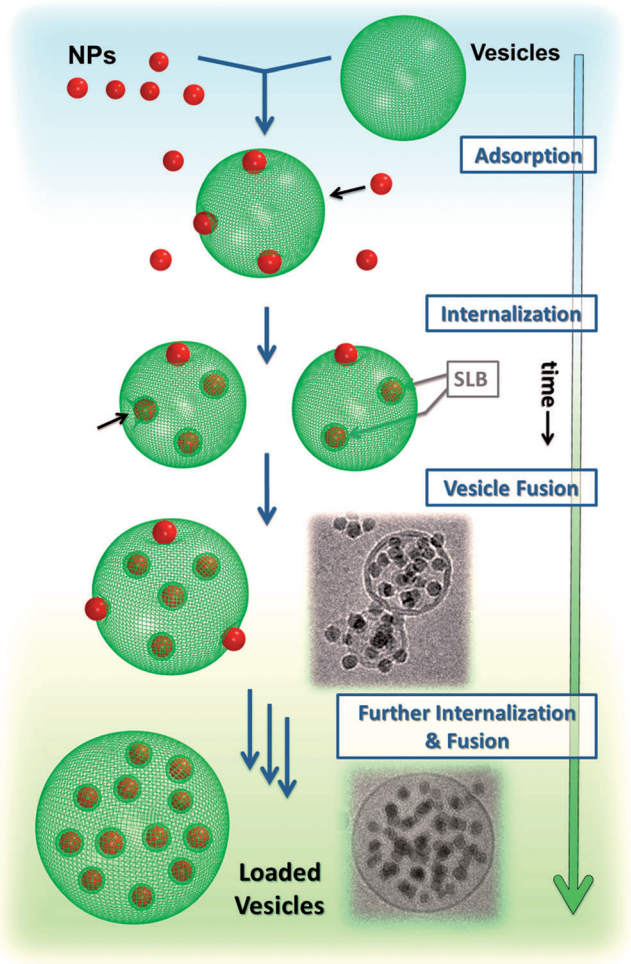

Figure 5. Schematic drawing of the structural progression resulting from the interactions between zwitterionic DOPC vesicles and SiNPs and the interplay of NP invagination and vesicle fusion (for comparison, corresponding cryo-TEM images for the various stages are shown).

of negatively charged SiNPs on the vesicle surface and allows to relax the curvature-induced stress on the vesicle membranes. In addition, more bilayer material becomes available for SLB formation during SiNP invagination and vesicle fusion increases the volume available within the vesicles (for a given membrane area). Hence, after fusion, further SiNPs can be incorporated and this process proceeds until the vesicles become so small again that further fusion is required. This circle of invagination of SiNPs and vesicle fusion is repeated until all of the SiNPs are finally incorporated within the vesicles which depends on the ratio [NP]/[vesicle]. Afterwards, a long-time metastable situation of nanoparticle-filled vesicles is achieved. The size of the final vesicles is rather constant and increases only somewhat for larger [NP]/[vesicle] ratios as now more NPs have to become incorporated per vesicle. For the case of constant vesicle size the number of NPs contained per final vesicle is simply given as ([NP]/[vesicle])/(1−β) and this simple formula is in good agreement with our experimental observations. It might also be noted that measuring the electric conductivity as a function of time did not show any significant changes (Figure S7), thereby indicating the chemical stability of the system and that ions are not released from the SiNPs.

In summary, this well-defined process leads to long-time stable hybrid colloids composed of SLB-covered SiNPs contained in phospholipid vesicles. This mechanism allows to produce structurally well-defined, uniform hybrid colloids, which can have a very high loading with SiNPs, depending on the [NP]/[vesicle] ratio. In addition, the SiNPs are protected by a SLB. This formation process should be generically applicable to phospholipid/nanoparticle systems, thus allowing the formation of interesting hybrid colloid systems that combine the cell membrane mimicking properties of vesicles with those of nanoparticles. Such hybrid colloids are interesting for applications where nanoparticles have to be hidden from the surroundings by having them encaged in a vesicle, thereby rendering it biocompatible. For instance one may load SiNPs with a drug molecule, thereby creating a smart delivery system, and similarly this should work for imaging or sensoring applications (where one may substitute the SiNPs by magnetic NPs). Finally, especially for low [NP]/[vesicle] ratios our findings shed light on the process of transporting NPs across phospholipid membranes and show that its kinetics slows down by increasing the NP concentration because of a process of self-inhibition arising from the mutual repulsion of adsorbed NPs.

Experimental Section

SLS and DLS experiments were done on an ALV/CGS-3 Compact Goniometer system with an ALV/LSE-5004 Light scattering Electronics multiple Tau Digital Correlator (ALV, Langen, Germany), using a 90° scattering angle and a 632 nm diode laser. All experiments were done in a thermostated toluene bath at 25 ± 0.1 °C. In the case of SLS, the scattering intensity was normalized using toluene as a reference, having a Rayleigh ratio of 1.34×10^{-5} cm^{-1} at 632.8 nm.

For cryo-TEM the samples were prepared on carbon-coated copper grids with a 200 mesh. Samples were prepared in a Vitrobot (FEI) at controlled temperature (25 °C) and humidity (100 % humidity). After blotting to a thin liquid film, a relaxation time of typically 20 seconds was applied, and then the grid was rapidly plunged in liquid ethane and vitrified. The sample was then studied in an FEI Tecnai G2 12 twin transmission electron microscope at 120 kV. The sample was kept at −175 °C or lower with a Gatan 626 cryo-specimen holder. Images were digitally recorded[14] with a Gatan UltraScan 1000 CCD camera at about three micrometers of underfocus. SANS experiments were performed on KWS-1 of JCNS in FRM-II, Garching, (Germany).

Received: July 6, 2014
Revised: August 3, 2014
Published online: September 26, 2014

Keywords: endocytosis · hybrid colloids · internalization · liposomes · nanoparticles

[1] a) R. Michel, M. Gradzielski, *Int. J. Mol. Sci.* **2012**, *13*, 11610–11642; b) P. R. Leroueil, S. A. Berry, K. Duthie, G. Han, V. M. Rotello, D. Q. McNerny, J. R. Baker, B. G. Orr, M. M. B. Holl, *Nano Lett.* **2008**, *8*, 420–424; c) P. R. Leroueil, S. Y. Hong, A. Mecke, J. R. Baker, B. G. Orr, M. M. B. Holl, *Acc. Chem. Res.*

2007, *40*, 335 – 342; d) S. Pierrat, E. Hartinger, S. Faiss, A. Janshoff, C. Sonnichsen, *J. Phys. Chem. C* **2009**, *113*, 11179 – 11183; e) Y. Roiter, M. Ornatska, A. R. Rammohan, J. Balakrishnan, D. R. Heine, S. Minko, *Nano Lett.* **2008**, *8*, 941 – 944; f) M. Schulz, A. Olubummo, W. H. Binder, *Soft Matter* **2012**, *8*, 4849 – 4864.

[2] a) D. V. Lynch, P. L. Steponkus, *Biochim. Biophys. Acta Biomembr.* **1989**, *984*, 267 – 272; b) A. S. Ulrich, M. Sami, A. Watts, *Biochim. Biophys. Acta Biomembr.* **1994**, *1191*, 225 – 230.

[3] J. Raedler, H. Strey, E. Sackmann, *Langmuir* **1995**, *11*, 4539 – 4548.

[4] O. Le Bihan, P. Bonnafous, L. Marak, T. Bickel, S. Trepout, S. Mornet, F. De Haas, H. Talbot, J. C. Taveau, O. Lambert, *J. Struct. Biol.* **2009**, *168*, 419 – 425.

[5] W. Helfrich, *Z. Naturforsch. C* **1973**, *28*, 693 – 703.

[6] a) H. G. Dobereiner, R. Lipowsky, *Europhys. Lett.* **1998**, *43*, 219 – 225; b) R. Lipowsky, H. G. Dobereiner, C. Hiergeist, V. Indrani, *Physica A* **1998**, *249*, 536 – 543.

[7] J. Pan, S. Tristram-Nagle, N. Kucerka, J. F. Nagle, *Biophys. J.* **2008**, *94*, 117 – 124.

[8] J. N. Israelachvili, *Intermolecular and Surface Forces*, 3rd ed., Academic Press, London, **2011**.

[9] a) K. Jaskiewicz, A. Larsen, I. Lieberwirth, K. Koynov, W. Meier, G. Fytas, A. Kroeger, K. Landfester, *Angew. Chem. Int. Ed.* **2012**, *51*, 4613 – 4617; *Angew. Chem.* **2012**, *124*, 4691 – 4695; b) K. Jaskiewicz, A. Larsen, D. Schaeffel, K. Koynov, I. Lieberwirth, G. Fytas, K. Landfester, A. Kroeger, *ACS Nano* **2012**, *6*, 7254 – 7262.

[10] R. Michel, T. Plostica, D. Danino, M. Gradzielski, *Soft Matter* **2013**, *9*, 4167 – 4177.

[11] a) N. Delorme, A. Fery, *Phys. Rev. E* **2006**, *74*, 030901; b) C. H. Lee, W. C. Lin, J. P. Wang, *Phys. Rev. E* **2001**, *64*, 020901.

[12] a) V. Tohver, J. E. Smay, A. Braem, P. V. Braun, J. A. Lewis, *Proc. Natl. Acad. Sci. USA* **2001**, *98*, 8950 – 8954; b) L. F. Zhang, S. Granick, *Nano Lett.* **2006**, *6*, 694 – 698.

[13] a) I. Bivas, A. G. Petrov, *J. Theor. Biol.* **1981**, *88*, 459 – 483; b) W. Helfrich, *Z. Naturforsch. Sect. A* **1978**, *33*, 305 – 315; c) W. Helfrich, *J. Phys.* **1985**, *46*, 1263 – 1268; d) A. G. Petrov, I. Bivas, *Prog. Surf. Sci.* **1984**, *16*, 389 – 512.

[14] a) D. Danino, *Curr. Opin. Colloid Interface Sci.* **2012**, *17*, 316 – 329; b) D. Danino, A. Bernheim-Groswasser, Y. Talmon, *Colloids Surf. A* **2001**, *183*, 113 – 122.

